

Theory of Localized Magnons in Ni^{++} -Doped Manganese Salts[†]

M. F. Thorpe

Brookhaven National Laboratory, Upton, New York 11973

(Received 3 March 1970)

There has been a series of optical experiments recently in which one or two magnons are created in the vicinity of a Ni^{++} impurity in RbMnF_3 , KMnF_3 , and MnF_2 . The single-magnon excitations can be understood using existing Green's-function theory. We find that this theory, which uses the Holstein-Primakoff transformation, is adequate for the host (spin $\frac{5}{2}$) but leads to certain difficulties at the impurity (spin 1), even in the present case where the impurity-host coupling is large. The line shape for the pair modes can be calculated when one of the two magnons is highly localized, thus allowing the three-body problem to be solved as an effective two-body problem. We show that if the lattice contains one magnon localized on the impurity itself, the impurity acts as though its spin were reduced from S' to $S' - 1$ (i.e., as a vacancy, in the case of Ni). Many of the experiments can be explained without a detailed knowledge of the Ni-Mn exchange, which is fortunate in the case of the rutile structure where it is probably complicated. We briefly discuss the g factors of the various modes and show that they can lead to useful information about the spatial extent of the excitations.

I. INTRODUCTION

The theory of localized magnons in insulating magnets has been discussed by many authors over the past few years for the case of a single isolated impurity. Previously, the study of localized phonon modes had been extensively developed following the pioneering work of Lifshitz.¹ The magnon problem has one advantage and one disadvantage from a theoretical point of view when compared to the corresponding phonon problem. In the phonon system one can usually make the harmonic approximation with a good deal of confidence, whereas in the spin system one cannot in general (one important exception is at very low temperatures in a ferromagnet). However, the localized magnons can be studied by keeping only the quadratic terms that arise when the Holstein-Primakoff transformation is performed on the spin operators. This is a good approximation for large values of the spin but leads to difficulties for low values of the spin (see for example a calculation by Parkinson² for a spin- $\frac{1}{2}$ impurity). We shall encounter these difficulties in our consideration of Ni^{++} (spin-1) impurities. The advantage the magnon problem has is that the number of parameters that appear is considerably reduced. For example, the properties of Ni-doped RbMnF_3 can be described by two parameters: the nearest-neighbor Mn-Mn and Ni-Mn exchange constants. In the typical phonon problem there are ≈ 10 unknown force constants that go into the determination of the local modes. In this paper, we have chosen to study manganese-fluoride antiferromagnets doped with nickel ions, for a number of reasons. The spin-wave spectra of the host manganese salts have been studied by inelastic neutron scattering, and the dispersion can well be described by only a few pa-

rameters. Many experimental data are also available using infrared and Raman scattering techniques to investigate the single- and two-magnon excitations in both the pure and doped systems. It is found that the nickel impurities are strongly coupled to the host manganese ions; this leads to certain modes being highly localized and simplifies the calculations.

The case of a single defect in a ferromagnet at zero temperature has been studied by Wolfram and Callaway,³ who obtain exact answers because the Hamiltonian can be diagonalized within the ground state and states with one spin deviation. The case of a defect in an antiferromagnet has been investigated by Lovesey,⁴ Tonegawa,⁵ and Tonegawa and Kanamori⁶ using a quadratic Bose Hamiltonian. We briefly sketch this calculation in Sec. II. The Ni-Mn exchange is greater than the Mn-Mn exchange by a factor of about 3.5. This means that the mode that is predominantly on the impurity site itself (the s_0 mode) is a long way above the spin-wave band in energy. The energy of this mode can also be calculated from an expansion about the cluster containing the impurity and its nearest neighbors on the opposite sublattice. We examine the denominator of the appropriate Green's function for large energies and compare this to the frequency of the s_0 mode obtained by diagonalizing the cluster Hamiltonian. The two approaches do not agree exactly because of the presence of spin deviations in the ground state of the antiferromagnet.

In Sec. VI, we examine the pair modes associated with a single defect. These are modes which are formed when the radiation field creates spin deviations on neighboring sites in the vicinity of the defect. Experimentally, these modes are identified as pair modes by doing a molecular field calcula-

tion, which is equivalent to just treating the Ising part of the Hamiltonian at low temperatures. Although this theory gives the position of the pair lines rather accurately, it does not give a width which comes from the S^+S^- terms in the Hamiltonian. The general problem is rather difficult, but we show that if one of modes is an s_0 mode, the impurity acts as if it had its spin reduced from S' to $S' - 1$ (i. e., it behaves as a vacancy or nonmagnetic impurity in the case of Ni^{++}). This turns out to be an excellent approximation for a strongly coupled impurity like Ni^{++} . A brief account of this solution to the three-body problem has been given elsewhere⁷ where it was applied to the perovskite structure. In this paper we also apply the theory to the rutile structure where the picture is complicated by the existence of more coupling parameters. However, because the Ni acts like a vacancy, one does not have to know much about the impurity-host coupling to be able to correlate a good many experimental results. We find that the pair modes are at lower frequencies than the sum of the frequencies of the individual modes. This attraction is similar to that found in pair modes in pure antiferromagnets.^{8,9} However, if both modes are on the impurity itself (i. e., two s_0 modes) we find a repulsion between the modes.

II. GREEN'S-FUNCTION THEORY OF LOCALIZED MODES

We consider a two-sublattice antiferromagnet with spin S and nearest-neighbor Heisenberg exchange J . The labels i and j denote the up and down sublattices, respectively,

$$H = \sum_{ij} J \vec{S}_i \cdot \vec{S}_j \quad (1)$$

This Hamiltonian may be solved for the spin-wave states using either equations of motions⁹ or the Holstein-Primakoff transformation.¹⁰ The magnon dispersion is given by

$$\omega_{\vec{k}} = JSz(1 - \gamma_{\vec{k}}^2)^{1/2}, \quad (2)$$

where

$$\gamma_{\vec{k}} = (1/z) \sum_{\vec{a}} e^{i\vec{k} \cdot \vec{a}}.$$

z is the number of nearest neighbors and \vec{a} is a vector connecting nearest neighbors. If we now add a substitutional defect, with spin S' and impurity-host exchange J' into the up sublattice, there will be an additional term in the Hamiltonian,

$$H' = \sum_{\Delta} [J'(\vec{S}'_0 \cdot \vec{S}_{\Delta}) - J(\vec{S}_0 \cdot \vec{S}_{\Delta})], \quad (3)$$

where Δ is a nearest neighbor to the defect which defines the origin labeled by zero. It is most convenient to transform to Holstein-Primakoff operators.¹⁰ For the up sublattice

$$S_i^+ = (2S - a_i^\dagger a_i)^{1/2} a_i, \quad (4a)$$

and for the down sublattice

$$S_j^- = b_j^\dagger (2S - b_j^\dagger b_j)^{1/2}. \quad (4b)$$

The other transformation equations between the spin operators and the Bose operators can be obtained by using $(S^*)^+ = S^-$ and the spin commutation relations.¹⁰ Expanding the square roots in Eq. (4) and keeping only the lowest-order terms, H' becomes

$$H' = JS \sum_{\Delta} [\phi (a_0^\dagger b_{\Delta}^\dagger + a_0 b_{\Delta}) + \epsilon a_0^\dagger a_0 + \rho b_{\Delta}^\dagger b_{\Delta}], \quad (5)$$

with

$$\begin{aligned} \phi &= (J'/J)(S'/S)^{1/2} - 1, \\ \epsilon &= (J'/J) - 1, \\ \rho &= (J'S'/JS) - 1. \end{aligned} \quad (6)$$

The Hamiltonian $H + H'$ [where H is also written in Bose operators, using Eq. (4) and keeping only the quadratic terms] can be diagonalized because the range of the interaction, H' , in real space is limited. The localized modes and resonances that result have been discussed by several authors⁴⁻⁶ and by Parkinson¹¹ with particular reference to the perovskite structure. The modes can be classified according to the paramagnetic point group of the defect. There will be an s_0 mode that is predominantly on the impurity, an s_1 mode that is predominantly on the near neighbors of the impurity, and various other non- s -like modes to give a total of $z + 1$. In the two structures with which we will be concerned, the perovskite will have s_0 , s_1 , p , and d modes¹¹ whereas the rutile structure has s_0 , s_1 , p , d , and f modes.⁴ (There are actually more modes in Ni:MnF_2 because the exchange is not simply nearest neighbor. This will be discussed more fully in Sec. VIII.)

We define Green's functions at $T = 0^\circ \text{K}$:

$$\langle\langle A, B \rangle\rangle = \frac{1}{2\pi} \sum_i \left(\frac{\langle 0|A|i\rangle \langle i|B|0\rangle}{\omega - (E_i - E_0)} - \frac{\langle 0|B|iX_i|A|0\rangle}{\omega + (E_i - E_0)} \right). \quad (7)$$

Then, in the pure system,

$$\langle\langle a_i; a_j^\dagger \rangle\rangle = \frac{1}{2\pi} G_0(\omega) = \frac{1}{2\pi N} \sum_{\vec{k}} \frac{e^{i\vec{k} \cdot \vec{r}_i - i\vec{k} \cdot \vec{r}_j}}{\omega^2 - \omega_{\vec{k}}^2} (\omega + JSz). \quad (8)$$

The poles of this Green's function occur at the spin-wave frequencies. When the impurity Hamiltonian H' [Eq. (5)] is included, the equations are modified and the Green's functions for the non- s -like modes become

$$G^{\text{sym}}(\omega) = \frac{G_0^{\text{sym}}(\omega)}{[1 - JS\rho G^{\text{sym}}(\omega)]}, \quad (9)$$

where ρ measures the strength of the perturbation caused by the impurity. The symmetrized Green's functions formed from Eq. (8) for the perovskite lattice are⁹

$$G_0^b(\omega) = (1/N) \sum_{\mathbf{k}} [2 \sin^2 k_x a(\omega + JSz) / (\omega^2 - \omega_{\mathbf{k}}^2)] ,$$

$$G_0^d(\omega) = \frac{1}{N} \sum_{\mathbf{k}} \frac{(\cos k_x a - \cos k_y a)^2}{\omega^2 - \omega_{\mathbf{k}}^2} (\omega + JSz) . \quad (10)$$

The equivalent expressions for the rutile structure are given in Sec. VIII. These Green's functions may be reexpressed in terms of those found in the theory of spin waves in ferromagnets (for details see Sec. VII in Elliott and Thorpe⁹) which have been tabulated by many authors.^{3,12,13} The condition for a bound state to occur above the band is $\rho > 0$, i. e., $J'S' > JS$.

The equations for the s -like modes are more complicated than Eq. (9) because the s_0 and s_1 modes mix. However, in the cases that we will consider, both modes occur above the spin-wave band and so we need to know only the denominator of the Green's function. The frequencies of these modes are given by the solution of¹¹

$$D_s(\pm\omega) = 0 , \quad (11)$$

where

$$D_s(\omega) = [\rho(\omega + JSz)^2 - (\rho + \epsilon)(\omega + JSz)JSz + \epsilon(JSz)^2] \\ \times (\omega - JSz)P_0(\omega) + (1 + \epsilon)JSz - \rho\omega \quad (12)$$

and

$$P_0(\omega) = (1/N) \sum_{\mathbf{k}} (\omega^2 - \omega_{\mathbf{k}}^2)^{-1} . \quad (13)$$

By examining the behavior of Eq. (12) we can see that the s_0 mode is above the spin-wave band if $J' > J$, whereas the s_1 mode is above if $J' > JS/(S' - S)$.

III. THEORY APPLIED TO Ni^{++} -DOPED RbMnF_3 AND KMnF_3

Both RbMnF_3 and KMnF_3 are good examples of two sublattice antiferromagnets with predominantly nearest-neighbor exchange. We shall see later when we consider MnF_2 that when the exchange is appreciable between more distant neighbors, numerical complications arise which tend to obscure the rather simple physics involved. The spin-wave dispersion curves for pure RbMnF_3 and KMnF_3 have been measured by inelastic neutron scattering^{14,15} and can be described by a nearest-neighbor Heisenberg model [Eq. (1)] with maximum spin-wave energies JSz of 71 and 76 cm^{-1} , respectively.¹¹ There is a slight canting of spins in KMnF_3 , which we neglect as it has a negligible effect on spin waves at the zone boundary where the density of states peaks.

A word of caution is required at this point. The ratio of the exchange between nearest-neighbor pairs and next-nearest-neighbor pairs is 0.29 in KMnF_3 ¹⁵ compared with only ± 0.06 in RbMnF_3 ,¹⁴ and so it might be supposed that a nearest-neighbor model would be inadequate in KMnF_3 . In fact, we have found a nearest-neighbor model to be satisfac-

tory because the density of states is dominated by a sharp peak near the zone boundary, and this can be well reproduced by a nearest-neighbor model if the exchange parameter is suitably chosen. The situation is very different in the rutile structure where the density of states develops two sharp peaks when next-nearest neighbor exchange is included. This point is further discussed in Sec. VIII.

Unfortunately, there are no measurements of the single s_1 , p , and d modes in these materials. However, there is an accurate measurement of the s_0 mode. Johnson, Dietz, and Guggenheim¹⁶ have studied the process in which an exciton on a Ni^{++} impurity decays into one or two s_0 magnons. This provides an excellent measurement of the energy of the s_0 mode, ω_{s_0} , and the energy of the pair of s_0 modes, $\omega_{s_0+s_0}$. There is no exciton-magnon interaction to complicate the situation, since the exciton and magnon do not coexist in time. They find ω_{s_0} to be 238 cm^{-1} in RbMnF_3 and 255.9 cm^{-1} in KMnF_3 .¹⁶ Using the expression Eq. (12) for the frequency of the s_0 mode, we can determine the value of J' as shown in the third column of Table I. It is instructive to examine Eq. (12) for large energies. $P_0(\omega)$ has no imaginary part above the spin-wave band and can be expanded as a power series in $[\omega^2 - (JSz)^2]^{-1}$,

$$P_0(\omega) = \frac{1}{N} \sum_{\mathbf{k}} \frac{1}{\omega^2 - \omega_{\mathbf{k}}^2} = \frac{1}{[\omega^2 - (JSz)^2]} \\ - \frac{(1/z)(JSz)^2}{[\omega^2 - (JSz)^2]^2} + \dots \quad (14)$$

It is only necessary to take the first two terms in the present case. Inserting Eq. (14) into Eq. (12), we find for large (J'/J) ,

$$\omega_{s_0} \simeq J'Sz - J'S' + JSS'(z-1)/(Sz - S') . \quad (15)$$

The first term $J'Sz$ is by far the largest and just that which would be obtained using molecular field

TABLE I. Comparison of the Green's-function theory and cluster model for the s_0 modes in the perovskite antiferromagnets RbMnF_3 and KMnF_3 with Ni impurities. $\Delta\omega = \omega_{s_0+s_0} - 2\omega_{s_0}$ is given slightly better by the cluster model when compared with experiment (Ref. 16). Missetich and Dietz (Ref. 16) have studied a slightly different cluster model further and obtain $\Delta\omega = 11.6$ and 12.5 for RbMnF_3 and KMnF_3 , which agrees even better with experiment.

	Expt		Green's-function theory		Cluster model	
	ω_{s_0}	$\Delta\omega$	J'	$\Delta\omega$	J'	$\Delta\omega$
RbMnF_3	238	10.9	16.7	13.1	15.9	12.4
KMnF_3	255.9	11.9	18	14.1	17.1	13.4

theory, i. e., by just taking the Ising terms in the Hamiltonian. To check the validity of Eq. (15), we put $\omega_{s_0} = 238 \text{ cm}^{-1}$ for RbMnF_3 and again find that $J' = 16.7 \text{ cm}^{-1}$; so that Eq. (15) forms a good approximation to the solution of Eq. (12) when the mode is well above the band. We note at this point that using the value of J' obtained from the s_0 mode, we can predict from Eq. (9) that the s_1 , p , and d modes should all occur between 2 and 4 cm^{-1} above the top of the spin-wave bands in RbMnF_3 and KMnF_3 . Of these, only the d mode in RbMnF_3 has so far been seen¹⁷ at 2 cm^{-1} above the band.

We digress at this stage to discuss the g factors of the single-magnon modes. Unfortunately, this is somewhat academic in the perovskites since the anisotropy is so extremely small that a spin-flop transition takes place upon application of a field. However, let us assume that we could introduce sufficient anisotropy (by straining the crystal for example) to allow the g factor to be measured. Explicitly we switch on an external field

$$-g\mu_B H \left[\sum_i S_i^z + \sum_j S_j^z \right] - g'\mu_B H S_0'^z + g\mu_B H S_0^z, \quad (16)$$

and ask for the linear shift in the frequency of the local modes. In practice, the modes will split as some impurities will be in one sublattice and some in the other. The g factor the p and d modes will be just g because these modes do not spread onto the impurity. If we rewrite Eq. (16) in terms of Bose operators and carry through the analysis of Sec. II, we get a modified expression for $D_s(\omega)$ [Eq. (12)]. If we again expand for large (J'/J) , we obtain

$$\omega_{s_0} \rightarrow \omega_{s_0} + g_{s_0} \mu_B H, \quad (17)$$

where

$$g_{s_0} = g' - (g - g')S' / (Sz - S'). \quad (18)$$

This result has an immediate physical interpretation. Remembering that the z component of the total spin of the system is a good quantum number and changes by one unit when a magnon is present in the lattice, we can write

$$g_{s_0} = g - (g' - g) (\langle s_0 | S_0'^z | s_0 \rangle - \langle 0 | S_0'^z | 0 \rangle), \quad (19)$$

where $|0\rangle$ is the ground state and $|s_0\rangle$ is the state with a single s_0 mode. Comparing Eqs. (18) and Eq. (19), we see that

$$\langle s_0 | S_0'^z | s_0 \rangle - \langle 0 | S_0'^z | 0 \rangle = -Sz / (Sz - 1'). \quad (20)$$

The expression (20) provides a good measure of the spatial extent of the s_0 excitation. In the present case

$$-Sz / (Sz - S') = -\frac{15}{14} = -1.07.$$

Had this number been exactly -1 , the s_0 mode would have been entirely on the impurity. The 7%

difference gives a good estimate of the probability of the excitation being on a host site.

In a ferromagnet, the coefficient of $(g - g')$ in Eq. (18) would give an exact measure of the delocalization of the s_0 mode. A problem arises in the antiferromagnet because the change in spin density due to the presence of an s_0 mode is positive at some sites and negative at others, and so the g factor does not give an exact measure of the spreading of the mode off the impurity site. However, the g factor as written in Eq. (19) does give one some information about the spatial extent of the s_0 mode. A detailed description would require the computation of the change in the average value of the z component of the spin at each site. This would be very lengthy and would not yield much insight.

IV. CLUSTER APPROXIMATION

The expressions that we have derived up until this point have only really been valid for large values of the spin. This is because the square roots in Eq. (4) were expanded in powers of $1/S$. This procedure should be reasonably good for Mn^{++} (spin $\frac{5}{2}$) but may not be so good for Ni^{++} (spin 1). To investigate this, we look at the local modes from a different point of view. When the impurity-host exchange is large, we can define $\vec{s} = \sum_{\Delta} \vec{S}_{\Delta}$ as the spin of the neighbors of the impurity and approximate $H + H'$ by H_{cl} where

$$H_{cl} = J' \vec{s} \cdot \vec{S}' + (z - 1) JS s^z. \quad (21)$$

The first term is the full interaction of the impurity with all its neighbors. It can be diagonalized to give a series of multiplets described by a spin \mathfrak{S} , where

$$\vec{\mathfrak{S}} = \vec{s} + \vec{S}'. \quad (22)$$

\mathfrak{S} goes from $s - S'$ to $s + S'$ [$s > S'$]. The second term in Eq. (21) represents the local field (due to the rest of the lattice) acting on the neighbors of the impurity. This should be a reasonably good approximation if J is sufficiently small when this term will be treated in first-order perturbation theory to remove all the degeneracy within the \mathfrak{S} multiplets. The ground state is the lowest level of the $\mathfrak{S} = s - S'$ multiplet, and the s_0 mode corresponds to a transition from the ground state to the lowest level of the $\mathfrak{S} = s - S' + 1$ multiplet. The energy of the s_0 mode, ω_{s_0} , is given by¹⁸ (putting $s = Sz$)

$$\omega_{s_0} = J' (Sz - S' + 1) - \frac{JS(z - 1) [(Sz - S') (1 - S') + 1]}{(Sz - S' + 1) (Sz - S' + 2)}. \quad (23)$$

We also calculate the g factor for this mode and obtain

$$g_{s_0} = g' + \frac{(g - g') [(Sz - S') (1 - S') + 1]}{(Sz - S' + 1) (Sz - S' + 2)}. \quad (24)$$

It is useful to compare these two expressions with Eqs. (15) and (18) obtained in Sec. III by use of the Holstein-Primakoff transformation. They clearly agree in the limit of large spins S and S' but are rather different for $S'=1$ owing to the existence of a factor $(1-S')$. Indeed, the last term in Eqs. (23) and (24) changes sign when one goes from the $S'=1$ case to the large S' limit.

Following the procedure of Sec. III, we can use Eq. (23) to give values of J' for Ni-doped RbMnF_3 and KMnF_3 . The results are shown in column 5 of Table I. The estimates of J' differ by about 5% from those obtained in Sec. III and given in column 3. This disagreement is $\sim \langle \delta S^z \rangle / S$, where $\langle \delta S^z \rangle$ is the spin deviation in the ground state of the antiferromagnet and is, of course, to be expected. The origin of the discrepancy is discussed in Ref. 19. Unfortunately, this disagreement is of the same order of magnitude as the interaction effects that occur when two local modes are excited simultaneously. The impasse is resolved to some extent by working consistently either within a cluster approximation or using the Holstein-Primakoff transformation with a Green's-function theory. This problem would not arise in a ferromagnet, of course, because the Holstein-Primakoff transformation gives the spin-wave energies correctly so that in the limit of large impurity-host coupling the cluster model and the Green's-function theory of the local modes would agree for *all* values of the spin. Comparing Eq. (24) with Eq. (19), we find

$$\langle s_0 | S_0'^z | s_0 \rangle - \langle 0 | S_0'^z | 0 \rangle = \frac{-(Sz - S')(Sz + 2) - 1}{(Sz - S' + 1)(Sz - S' + 2)} \quad (25)$$

Using $S = \frac{5}{2}$, $z = 6$, $S' = 1$, the expression Eq. (25) becomes $-\frac{15}{16} = -0.94$. (This should be compared to -1.07 obtained in Sec. III.) The fact that the two methods give estimates on the opposite sides of -1.0 should not trouble the reader. The change in the expectation value of the magnetization at a site, due to the presence of an s_0 magnon, can have either sign, depending on the sublattice; and so the total change in the magnetization of the host can also be of either sign. The important point is that both methods give results near to -1.0 , showing that the mode is highly localized.

To conclude this section, we calculate the energy and g factor of the pair $s_0 + s_0$ mode within the cluster Hamiltonian [Eq. (21)]. This mode is a transition from the ground state to the lowest level of the multiplet with $\mathfrak{S} = S - S' + 2$. Using the same method of calculation as for the single s_0 mode, we find that

$$\omega_{s_0 + s_0} = J(2Sz - 2S' + 3) - \frac{JS(z-1)[(Sz - S')(3 - 2S') + 3]}{(Sz - S' + 1)(Sz - S' + 3)} \quad (26)$$

and

$$g_{s_0 + s_0} = 2g' + (g - g') \frac{[(Sz - S')(3 - 2S') + 3]}{(Sz - S' + 1)(Sz - S' + 3)} \quad (27)$$

The energy of the transition $s_0 + s_0$ is greater than twice the energy of a single s_0 transition (i.e., there is a repulsive interaction between the two modes). It is useful to define

$$\Delta\omega = \omega_{s_0 + s_0} - 2\omega_{s_0} = J' - \frac{JS(z-1)[(Sz - S')(Sz + S' + 1)]}{(Sz - S' + 1)(Sz - S' + 2)(Sz - S' + 3)} \quad (28)$$

Using the value of J' calculated from the s_0 mode [Eq. (23)] and shown in column 5 of Table I, we can calculate $\Delta\omega$. This is done in column 6 of Table I, and may be compared with the experimental value in column 2. The agreement is quite satisfactory. The repulsive interaction between the two s_0 modes is a consequence of the antiferromagnetic coupling between host and impurity. It would be attractive for a ferromagnetically coupled impurity. Usually, interactions between magnons are attractive because they come predominantly from the Ising terms in the Hamiltonian. The interaction between the s_0 modes is quite different in character, and arises from the S^+S^- terms in the Hamiltonian (i.e., in an Ising system there would be no interaction between two s_0 modes). A cluster method was first used by Misetich and Dietz¹⁶ who show that by taking larger clusters around the impurity than we have considered here, agreement between theory and experiment can be still further improved (see comment under Table I). In this method, the S^+S^- terms in the Hamiltonian are treated as a perturbation on the Ising energies. More distant neighbors of the impurity enter into the calculation in each higher order of perturbation theory and their method can legitimately be called a cluster method also.

The cluster model is rather good for s_0 modes which only interact weakly with the host spin waves. However, it is much poorer for other modes, particularly those, near the band edge, that spread considerably into the host. It is, of course, of no use in describing resonances within the band, as it fails to give a width. Having said this, one must admit that it has been applied with considerable success by Dietz *et al.*²⁰ to get the central position of many single- and two-magnon line shapes. In complicated situations (e.g., Co^{++} impurities where orbital effects complicate the exchange), the method of Dietz *et al.* can yield useful information about the coupling of an impurity to the host. However, in simple cases where the interactions are known, it is possible to do considerably better, as we will show in Sec. V.

V. INTERACTION OF LIGHT WITH THE MAGNETIC SYSTEM

In this section, we will discuss the interaction of the radiation with the magnetic system that results in the excitation of single and pairs of localized modes. The mechanisms are the same as in the pure crystal, but the form (i. e., the symmetry) of the interactions is changed due to the reduction in symmetry caused by the presence of an impurity. The single-magnon localized modes with appropriate symmetry should be observable as a magnetic dipole transition. The form of this interaction is simply

$$H_{\text{MD}} = \mu_B \vec{H} \cdot \sum_i g_i \vec{S}_i, \quad (29)$$

where \vec{H} is the magnetic field of the radiation. The summation over all the sites i contains a factor g_i which allows for the g factor of host and impurity to be different. The presence of the impurity breaks the translational symmetry, and so magnons of all \vec{k} vectors may be excited. The infrared absorption cross section is obtained by treating H_{MD} in the Born approximation. The Raman cross section is more complicated and is an electric dipole transition that may be calculated by using the spin-orbit coupling in an excited state.²¹ The single-magnon modes are also observable with neutrons (e. g., Co^{++} in MnF_2),²² but no observations on Ni^{++} impurities in manganese salts have yet been reported.

The pair modes are allowed as an electric dipole transition.^{21,23} In many instances, the form of the interaction of the radiation field with the magnetic system will be the same as in the pure system, although the actual constants appearing in the interaction Hamiltonian will be different. However, extra terms are allowed in the interaction in the perovskite structure because pairs of ions near to the impurity no longer have a center of inversion. The coupling of pairs of ions probably takes place via an exchange interaction involving intermediate states of the pair. In spin-only systems like Mn^{++} and Ni^{++} , we expect terms in $\vec{S}_i \cdot \vec{S}_j$ to be dominant, and so the interaction responsible for the Raman scattering of light with electric vector \vec{E} into light with electric vector \vec{E}' will have the form

$$H_{\text{Raman}} = \sum_{i,j} [B_{ij}^3 (\vec{E} \cdot \hat{\delta}) (\vec{E}' \cdot \hat{\delta}) + (B_{ij}^1 - \frac{1}{3} B_{ij}^3) (\vec{E} \cdot \vec{E}')] \times \vec{S}_i \cdot \vec{S}_j, \quad (30)$$

where $\hat{\delta}$ is a unit vector along $\vec{i} - \vec{j}$ connecting nearest neighbors. In the pure crystal,⁹ the B_{ij}^1 , B_{ij}^3 were independent of i, j because of the translational invariance of the lattice. The terms in B_{ij}^1 give rise to scattering with over-all s symmetry (Γ_1^+ in the cubic group²⁴), i. e., such modes as s_0

+ s_1 and $s_0 + s_0$. The latter mode will have small intensity, however, as the Hamiltonian [Eq. (30)] creates deviations on neighboring sites, whereas the two deviations in the $s_0 + s_0$ mode spend most of their time on the same site. Calculations show that the $s_0 + s_1$ mode does not have any resonant behavior and is just a broad background mode. The terms in B_{ij}^3 give rise to scattering with over-all d symmetry (Γ_3^+ in the cubic group), i. e., $s_0 + d$. Two p modes on the neighbors of an impurity contain a d -like representation but will not be excited strongly by Eq. (30) which only couples nearest neighbors. Nearest neighbors of the impurity are not themselves nearest neighbors in the perovskite lattice.

The interaction responsible for infrared absorption in the pure crystal does not contain a term in $\vec{S}_i \cdot \vec{S}_j$ and so will be small.⁹ Such a term may occur in the doped crystal, however.¹¹ It will have the form

$$A \sum_{\Delta} (\vec{E} \cdot \vec{\Delta}) \vec{S}_0' \cdot \vec{S}_{\Delta}. \quad (31)$$

This will give rise to absorption with p symmetry (Γ_4^- in the cubic group) of which the most important component will be the $s_0 + p$ mode.

Arguments similar to those given in the previous paragraph can be used in the rutile structure to obtain the interactions in doped systems from those in the pure system.⁹ The modifications are less important than in the perovskites as two magnetic ions in the rutile structure do not have a center of inversion even in the pure crystal. From the discussion of this section, we expect modes of the type $s_0 + \alpha$, where α is predominantly on the near neighbors of the impurity, to be most strongly excited. Experimentally, these are the only modes to have been observed thus far, to the best of the author's knowledge. Fortunately, these are by far the simplest to treat theoretically, as we will show in Sec. VI.

VI. GREEN'S-FUNCTION THEORY OF THE PAIR MODES

The general problem of calculating the two-magnon modes in the presence of an impurity is very complex, because one is involved with two magnons propagating in an external field, i. e., a three-body problem. For a ferromagnet, it is possible to write down a closed set of equations within the states of two-spin deviations. For an antiferromagnet, this is also possible if plausible assumptions about the ground state are made. However, unlike the pure case,^{9,25} it is not possible to solve these equations when an impurity is present, unless some approximations are made. If one of the magnons is well localized, the spin deviation associated with that mode will have a large amplitude

only on a limited number of sites in the vicinity of the impurity. If we solve the intermediate problem of the original impurity plus the spin deviations caused by the presence of the first magnon around the impurity for the one-magnon states, a solution to the problem may be obtained. This is always true in principle; in practice the problem can only be handled if the first magnon has a large amplitude at a small number of sites near the impurity.

Thus, the problem of finding the two-magnon states in a single-impurity system can be reformulated in terms of the simpler problem of finding the one-magnon states associated with a number of impurities in a cluster. To make these statements more meaningful, let us consider the case of most interest, i. e., the $s_0 + \alpha$ modes. If we operate on the ground state with $S_0'^+$, we create an s_0 mode and band modes with over-all s symmetry:

$$S_0'^+ |0\rangle = \alpha_0 a_{s_0}^\dagger |0\rangle + \sum_{\mathbf{k}} \alpha_{\mathbf{k}}^\dagger \alpha_{\mathbf{k}}^\dagger |0\rangle, \quad (32)$$

where the α 's measure the amplitude of the various modes, the summation is over the whole Brillouin zone with all the $\alpha_{\mathbf{k}}$ within the star of \mathbf{k} equal, and the a^\dagger are single-magnon creation operators. For calculation of the $s_0 + \alpha$ mode, we are only interested in the first term in Eq. (32), which acts as an intermediate ground state $|I\rangle$ for the creation of the second-magnon:

$$|I\rangle = a_{s_0}^\dagger |0\rangle = \frac{\beta_0 S_0'^+ |0\rangle}{(2S_0')^{1/2}} + \frac{\beta' \sum_{\Delta} S_{\Delta}^+ |0\rangle}{(2S_{\Delta}')^{1/2}} + \text{etc.} \quad (33)$$

The higher terms in Eq. (33) are spin deviations on more distant neighbors of the impurity, having s symmetry. The cross section for Raman scattering and infrared absorption may be obtained from the Fermi Golden Rule formula. This cross section for the $s_0 + \alpha$ mode will be proportional to $S^{s_0 + \alpha}(\omega)$ given by

$$S^{s_0 + \alpha}(\omega) = 2\pi \sum_i |\langle i | \sum_{\Delta} f_{\alpha}(\Delta) S_{\Delta}^+ S_0'^+ |0\rangle|^2 \delta(\omega - E_i + E_0). \quad (34)$$

The summation over Δ includes a factor $f_{\alpha}(\Delta)$ to select the correct weighting factor for the α mode. (The equivalent factor for the s_0 mode multiplying $S_0'^+$ is just 1.) Using Eqs. (32) and (33), the cross section for the $s_0 + \alpha$ mode may be rewritten

$$S^{s_0 + \alpha}(\omega) = 2\pi |\alpha_0|^2 \sum_i |\langle i | \sum_{\Delta} f_{\alpha}(\Delta) S_{\Delta}^+ |I\rangle|^2 \delta(\omega - E_i + E_0). \quad (35)$$

We define

$$\tilde{S}^{\alpha}(\omega) = 2\pi \sum_i |\langle i | \sum_{\Delta} f_{\alpha}(\Delta) S_{\Delta}^+ |I\rangle|^2 \delta(\omega - E_i + E_I), \quad (36)$$

where E_I is the energy of the state $|I\rangle$. It is clear that

$$S^{s_0 + \alpha}(\omega) = |\alpha_0|^2 \tilde{S}^{\alpha}(\omega - E_I + E_0). \quad (37)$$

The convenience of this representation of the cross section is that $\tilde{S}^{\alpha}(\omega)$ can be obtained from a single-particle Green's function of the type Eq. (7), where the true ground state is replaced by the intermediate ground state $|I\rangle$. Equations (34) and (37) are merely a reformulation of the problem. However, we are now forced into making some approximations even if $|I\rangle$ differs from $|0\rangle$ only on a limited number of sites. We consider first the case of a ferromagnetically coupled impurity in a ferromagnetic host [a system described by the Hamiltonian $-H-H'$ given in Eqs. (1) and (3)]. If we are calculating the spin-wave excitations from the true ground state $|0\rangle$, we can use the method of calculation in which $[S^-, H]$ is allowed to act on the ground state. In the absence of an impurity,

$$\begin{aligned} i \frac{\partial}{\partial t} S_i^- |0\rangle &= [S_i^-, H] = \sum_j J_{ij} (S_j^+ S_i^- - S_j^- S_i^+) |0\rangle \\ &= \sum_j J_{ij} S_j^- (S_i^+ - S_i^-) |0\rangle. \end{aligned} \quad (38)$$

Equations of the type (38) lead to the correct single-magnon energies in both the pure and single-impurity cases. However, for the present we are looking for excitations from the intermediate state $|I\rangle$, and thus Eq. (38) is replaced by the approximate equation

$$\begin{aligned} i \frac{\partial}{\partial t} S_i^- |I\rangle &= [S_i^-, H] |I\rangle = \sum_j J_{ij} (S_j^+ S_i^- - S_j^- S_i^+) |I\rangle \\ &\approx \sum_j J_{ij} (\langle I | S_i^+ | I \rangle S_j^- - \langle I | S_j^+ | I \rangle S_i^-) |I\rangle. \end{aligned} \quad (39)$$

We see that within this random-phase approximation, each spin acts as if it had a value $\langle I | S_i^+ | I \rangle$, i. e., its expectation value in the intermediate ground state $|I\rangle$: $\langle I | S_i^+ | I \rangle \leq |S_i|$ where in the impurity case the equal sign will hold outside a range that characterizes the spatial extent of the spin deviations in the intermediate ground state $|I\rangle$.

In the antiferromagnet, we also encounter the problem of the existence of spin deviations even in the true ground state $|0\rangle$. However, equations of motion of the type (38) are, where S_i^z acting on the ground state is replaced by $\pm S$, equivalent to performing the Holstein-Primakoff transformation and to keeping only the quadratic terms. It is therefore reasonable to expect that equations of the type (39), where S_i^z acting on $|I\rangle$ is replaced by $\langle I | S_i^z | I \rangle$, will give a good account of excitations from the state $|I\rangle$. This approximation assumes that the pair modes are not very sensitive to the precise pattern of spin deviations around the impurity in the ground state. Experience leads one to believe that this is correct and the good agreement between theory and experiment obtained in Secs. VII and VIII reinforces this assertion.

The problem of finding the single-magnon states around a cluster of impurities has not been tackled.

It is straightforward in principle, but will involve the diagonalizing of rather large matrices. It has been solved for the case of two adjacent and identical impurities in a fcc ferromagnet by Frikkee²⁶ and also for two impurities with arbitrary separation in a ferromagnetic linear chain by White and Hogan.²⁶ The effect of the neighboring impurities is to split the single-impurity modes. Fortunately, this ambitious computational program does not have to be carried out for the case of Ni⁺⁺ impurities in manganese salts and very probably other situations (e.g., Fe⁺⁺ in MnF₂). The s_0 mode is highly localized on the impurity. According to the work of Sec. III, it has only a 7% probability of being off the Ni⁺⁺. The cluster methods of Sec. IV give a similar estimate of this probability. Thus, to a very good approximation we can put $|\beta_0|^2 = 1$ in Eq. (33) and say that the quantities

$$\langle I | S_i^z | I \rangle = \langle s_0 | S_i^z | s_0 \rangle \simeq \pm S$$

and

$$\langle I | S_0^z | I \rangle = \langle s_0 | S_0^z | s_0 \rangle \simeq S' - 1$$

for the impurity. Using these decoupling parameters in equations of the type (39), we can say that the impurity acts as if its spin were reduced from S' to $S' - 1$ for the formation of the second magnon. That is, *the Ni impurity acts as if it were a vacancy (i. e., a nonmagnetic defect) when the lattice contains one s_0 excitation.* We will find that the above approximation gives a very good account of the experiments described in Secs. VII and VIII. The terms that we have neglected, i. e., the term in β' , and higher order in Eq. (33) should (a) broaden the pair mode slightly and (b) introduce small broad peaks at other frequencies.

VII. PAIR MODES IN Ni-DOPED RbMnF₃ AND KMnF₃

We apply the theory in Sec. VI to the simplest case in which experimental results are available, i. e., Ni⁺⁺-doped RbMnF₃ and KMnF₃. We repeat a warning given in Sec. IV, that one must work consistently within either a cluster-type theory or a Green's-function theory to describe the interaction effects correctly. In this section and Sec. VIII, we work with the Bose operators in a Green's-function theory. This is because the width of the pair modes is important, and it is almost impossible to get a width starting from a cluster approximation, because no attempt is made to treat the host magnons.

The energy of a single s_0 mode ω_{s_0} is given by Eq. (12). When this mode is excited, the lattice is in the intermediate ground state in which the Ni⁺⁺ acts as a nonmagnetic impurity ($S' = 0$). However, if we put $S' = 0$, but $J' \neq 0$ in $H + H'$ given in Eqs. (1) and (5), we find that a term still exists:

$$J' S z a_0^\dagger a_0 \quad (40)$$

This is the only term involving operators on the impurity site, and so it corresponds to the energy of the second s_0 mode:

$$\omega_{s_0+s_0} - \omega_{s_0} = J' S z \quad (41)$$

It would, therefore, be more accurate to say that the Ni acts as a vacancy unless the second mode is an s_0 mode. Physically, this must be, since one can certainly create two deviations in the Ni which has spin 1. [It may be noted that Eq. (41) may be obtained from Eq. (15) by putting $S' = 0$.] Using Eq. (41) and the values of S' derived earlier (Table I), we can compute $\Delta\omega = \omega_{s_0+s_0} - 2\omega_{s_0}$. The result is shown in column 4 of Table I. It can be seen that the agreement with experiment is good. It is instructive to use the approximate form for ω_{s_0} [Eq. (15)] that is valid for large (J'/J) . Using also Eq. (41) and putting $S' = 1$ we find that

$$\Delta\omega \simeq J' - JS(z-1)/(Sz-1) \quad (42)$$

Remembering that $Sz = 15$, both Eqs. (42) and (28) are well approximated by

$$\Delta\omega \simeq J' - J(z-1)/z \quad (43)$$

This result has previously been obtained by Misetch and Dietz¹⁶ (expanding the denominator in their expression for $\delta'E$ for large J_a/J_b). The fact that Eq. (43) is valid within either scheme of calculation gives credence to the assertion that the interaction effects can be obtained, provided one works consistently within either scheme of calculation.

We now calculate the line shapes for the $s_0 + p$ and $s_0 + d$ modes using the equations of Sec. VI. $\tilde{S}^\alpha(\omega)$ for a p or d mode around a vacancy is given by [see Eq. (9)]

$$\tilde{S}^\alpha(\omega) = 2 \operatorname{Im} \left\{ \frac{G_0^\alpha(\omega)}{[1 + JS G_0^\alpha(\omega)]} \right\} \quad (44)$$

and thus,

$$S^{s_0+\alpha}(\omega) = 2 |\alpha_0|^2 \operatorname{Im} \left(\frac{G_0^\alpha(\omega - \omega_{s_0})}{1 + JS G_0^\alpha(\omega - \omega_{s_0})} \right) \quad (45)$$

The only place that the Ni-Mn exchange J' enters Eq. (45) is through ω_{s_0} . We use the experimentally measured value of ω_{s_0} (Table I) and compute Eq. (45) for the $s_0 + d$ mode, using the expression Eq. (10) for G_0^d . The results are shown in Fig. 1. There are no adjustable parameters in the theory except the peak height which is adjusted to agree with experiment.²⁷ The slight broadening of the experimental line shape may be mostly instrumental (the resolution is $\sim 3 \text{ cm}^{-1}$) and the lines have not been resolution corrected. Also plotted on the same diagram is a δ function at $\omega_{s_0} + \omega_d$ (representing the scattering that would be observed if there were no magnon-magnon interaction). ω_d is calculated from

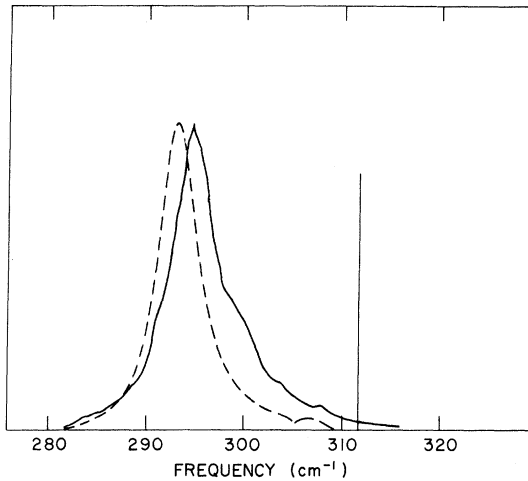


FIG. 1. Raman scattering from Ni:RbMnF₃ (Ref. 27) using unpolarized light. The instrumental width is about 3 cm⁻¹. The dashed theoretical curves for the $s_0 + d$ mode contain no free parameters except the peak height, which is adjusted to agree with experiment. The line at 312 cm⁻¹ represents a δ function at the energy $\omega_{s_0} + \omega_d$ (i. e., excluding the magnon-magnon interaction). The kink in the theoretical curve is due to the X magnons (Ref. 9).

Eq. (9) using J' from column 3 of Table I. The effect of the magnon-magnon interaction is clear. The δ function is shifted downwards by $\sim J'$ and broadened. Although the s_0 and d modes are separately localized (i. e., δ functions), the pair mode has a width because the presence of the s_0 mode allows the d mode to propagate through the lattice; this is in contrast to the $s_0 + s_0$ mode which does not propagate through the lattice and so remains a δ function (i. e., the two s_0 modes form a bound pair that remain in the vicinity of the impurity). In Fig. 2, we give a similar comparison of theory and experiment²⁸ for KMnF₃.

As mentioned in Sec. V, the odd-parity modes are not excited in the pure crystal because of the inversion symmetry, but should be allowed in the doped sample. By the methods above, we calculate that for RbMnF₃ and KMnF₃ the $s_0 + p$ modes should be centered at 291 and 313 cm⁻¹ with widths 15 and 16 cm⁻¹, respectively. These modes are therefore just below the corresponding $s_0 + d$ modes and much broader. Unfortunately, these modes are not observable because the crystals become nearly opaque to infrared radiation at these frequencies owing to phonon absorption.²⁹

VIII. PAIR MODES IN Ni-DOPED MnF₂

Impurities in the rutile structure are much more complicated objects than in the perovskite structure. There are two reasons for this. The first

is that the host and impurity cannot be characterized by a single-exchange parameter each. The second is that including an impurity in the lattice divides the eight neighbors of the impurity on the opposite sublattice into two groups of four with different exchanges to each. (For a full discussion of this, see Shiles and Hone.³⁰) Although these complications are mainly computational in that they do not give rise to any great qualitative changes in the local modes, etc., they nevertheless present a formidable problem that has not yet been satisfactorily resolved in that the exchange coupling between Ni and Mn in Ni:MnF₂ is not accurately known.

The host spin waves may be well described by three parameters: J_1 a coupling to the two neighbors along the c axis in the same sublattice, J_2 a coupling to the eight neighbors on the opposite sublattice, and an anisotropy field H_A . These parameters have been chosen by Tonegawa⁵ to give a good fit to the spin-wave dispersion curves^{31, 32}

$$J_1 = 0.44 \text{ cm}^{-1}, J_2 = 2.48 \text{ cm}^{-1}, H_A = 0.8 \text{ cm}^{-1}. \quad (46)$$

Note the difference of a factor of 2 between our definition of the exchange integrals and that used by both Tonegawa and a previous paper.³³ Although the ratio J_1/J_2 is smaller than in KMnF₃, we cannot neglect J_1 in this case. Exclusion of J_1 means that the system becomes effectively cubic,⁹ whereas the inclusion of J_1 produces two sharp peaks in the density-of-states characteristic of a uniaxial crystal, and this produces clearly observable effects in the optical spectra.³³ The magnon dispersion is given by

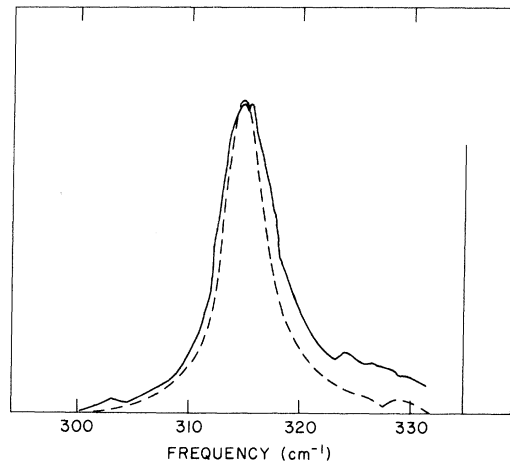


FIG. 2. Same as Fig. 1 but for Ni:KMnF₃. The experimental results are those of Ref. 28. The δ function at $\omega_{s_0} + \omega_d$ is at 335 cm⁻¹.

$$\omega_{\mathbf{k}}^2 = [8J_2S + H_A - 4J_1S \sin^2(\frac{1}{2}k_x c)]^2 - [8J_2S \cos(\frac{1}{2}k_x a) \cos(\frac{1}{2}k_y a) \cos(\frac{1}{2}k_z c)]^2. \quad (47)$$

The inclusion of these extra parameters in the magnon dispersion complicates the unperturbed Green's functions slightly. Equation (8), which is valid for a nearest-neighbor Heisenberg exchange Hamiltonian, becomes

$$\langle\langle a_i; a_j^\dagger \rangle\rangle = \frac{1}{2\pi} G_0(\omega) = \frac{1}{2\pi N} \sum_{\mathbf{k}} \frac{e^{i\mathbf{k} \cdot \vec{r}_i - \vec{r}_j} [\omega + 8J_2S + H_A - 4J_1S \sin^2(\frac{1}{2}k_x c)]}{\omega^2 - \omega_{\mathbf{k}}^2}. \quad (48)$$

$$G_0^{dxz}(\omega) = G_0^{dyz}(\omega) = \frac{1}{N} \sum_{\mathbf{k}} \frac{8 \cos^2(\frac{1}{2}k_x a) \sin^2(\frac{1}{2}k_y a) \sin^2(\frac{1}{2}k_z c) [\omega + 8J_2S + H_A - 4J_1S \sin^2(\frac{1}{2}k_x c)]}{(\omega^2 - \omega_{\mathbf{k}}^2)}, \quad (49)$$

$$G_0^{xy}(\omega) = \frac{1}{N} \sum_{\mathbf{k}} \frac{8 \sin^2(\frac{1}{2}k_x a) \sin^2(\frac{1}{2}k_y a) \cos^2(\frac{1}{2}k_z c) [\omega + 8J_2S + H_A - 4J_1S \sin^2(\frac{1}{2}k_x c)]}{(\omega^2 - \omega_{\mathbf{k}}^2)}, \quad (50)$$

$$G_0^f(\omega) = \frac{1}{N} \sum_{\mathbf{k}} \frac{8 \sin^2(\frac{1}{2}k_x a) \sin^2(\frac{1}{2}k_y a) \sin^2(\frac{1}{2}k_z c) [\omega + 8J_2S + H_A - 4J_1S \sin^2(\frac{1}{2}k_x c)]}{(\omega^2 - \omega_{\mathbf{k}}^2)}. \quad (51)$$

The cross section for the $s_0 + \alpha$ modes where α is of d or f symmetry is proportional to $S^{s_0+\alpha}(\omega)$ given by

$$S^{s_0+\alpha}(\omega) = 2 |\alpha_0|^2 \text{Im} \left(\frac{G_0^\alpha(\omega - \omega_{s_0})}{1 + J_2 S G_0^\alpha(\omega - \omega_{s_0})} \right). \quad (52)$$

We see again that the only place the Ni-Mn exchange enters this expression is through ω_{s_0} which has been measured by Missetich and Dietz¹⁶ to be 120.4 cm^{-1} . Using the crystal Green's functions (49)–(51) of Tonegawa,⁵ we compare the calculated modes $s_0 + d_{xz}$, $s_0 + d_{yz}$, $s_0 + d_{xy}$, and $s_0 + f$ with experiment^{34, 35} in Figs. 3–5, respectively. The agreement is rather good considering there are no adjustable parameters except the peak height in Eq. (52). Theory predicts the center of the peaks in Figs. 3–5 to be at 166.7, 164.4, and 167.3 cm^{-1} , respectively, whereas experiment gives 167.0, 164.5, and 167.5 cm^{-1} . Also, the widths are predicted to be 3.5, 3.0, and 1.4 cm^{-1} and experimentally they are 7.1, 5.7, and 2.5 cm^{-1} . The peak heights agree very well and the widths are well correlated, although the experimental widths are much larger than our theory gives. As with the perovskites, this is probably mostly resolution ($\sim 3 \text{ cm}^{-1}$) but may reflect some deficiencies in the theory.

The same theory can also be applied to Fe^{++} impurities in MnF_2 using the appropriate ω_{s_0} (measured by Weber³⁶) in Eq. (52) and replacing J_2S by $J_2S - J'_2(S' - 1)$, where $S' = 2$ in this case, and we will assume that the Fe-Mn exchange can be described by a single parameter J'_2 . If the Fe-Mn exchange

We can now calculate the spectral weight function $S^\alpha(\omega)$ for a vacancy as was done for the perovskite structure in Sec. VII. Because of the J_1 coupling in the host, two new representations are introduced: one with s -like (Γ_1^+) symmetry and the other with p -like (Γ_2^+) symmetry under the group D_{4h} . However, we are only interested in the d -like modes (Γ_4^+ and Γ_5^+) excited in Raman scattering and f -like modes (Γ_3^+) excited in infrared absorption experiments. The expressions for these modes are given by the same expression used in Sec. VII [Eq. (44)] where the $G_0^\alpha(\omega)$ is the symmetrized Green's functions formed from Eq. (48)

is more complicated, as it probably is, the expression (52) will become even more complex. The Fe impurity, therefore, acts as if it had spin 1 for the creation of the α magnon in the pair $s_0 + \alpha$. This is a poorer approximation because the Fe-Mn exchange is much weaker than the Ni-Mn exchange so that the s_0 mode is not so far above the spin-wave band and not so localized. Nevertheless, the main features of the Fe:MnF_2 spectra are readily explainable. The $s_0 + d_{xz}$ mode is a few cm^{-1} above the $s_0 + d_{xy}$ mode and has a greater width. We do not attempt a detailed comparison between theory and experiment, however, as the position of the peak moves almost linearly with $J_2S - J'_2(S' - 1)$. Thus, an error of 2 cm^{-1} in the position of the center of the line would give a value of J'_2 different by 2 cm^{-1} . This is an enormous percentage error as $J'_2 \sim 4 \text{ cm}^{-1}$. This underlines again the fact that most of the dependence of the pair modes on the impurity-host exchange enters into expressions like Eq. (45) through ω_{s_0} (entirely, in the case $S' = 1$). We conclude, therefore, that the single-magnon modes are far more useful in determining the impurity-host exchange than are the pair modes.

IX. g FACTOR OF PAIR MODES

The two-magnon modes in a pure antiferromagnet are not affected by a magnetic field at low temperatures. This is because

$$[S_1^z + S_2^z, \vec{S}_1 \cdot \vec{S}_2] = 0 \quad \text{and} \quad [\sum_i S_i^z, H] = 0, \quad (53)$$

where H is the Heisenberg Hamiltonian given in Eq.

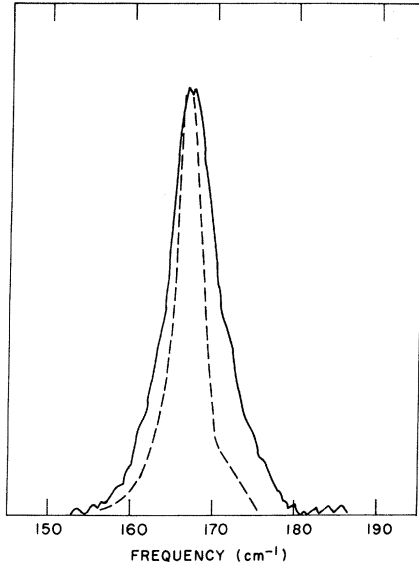


FIG. 3. Raman mode $s_0 + d_{xy}$ or $s_0 + d_{xz}$ from Ni:MnF₂. The experimental data are from Ref. 34. The solid line is experimental and the dashed line theoretical.

(1) and the summation is over all sites. Another way of saying this is that the radiation creates one magnon on each sublattice. When a field is applied, the energy of a magnon is changed by $+\mu_B g H$ on one sublattice and $-\mu_B g H$ on the other and so that the

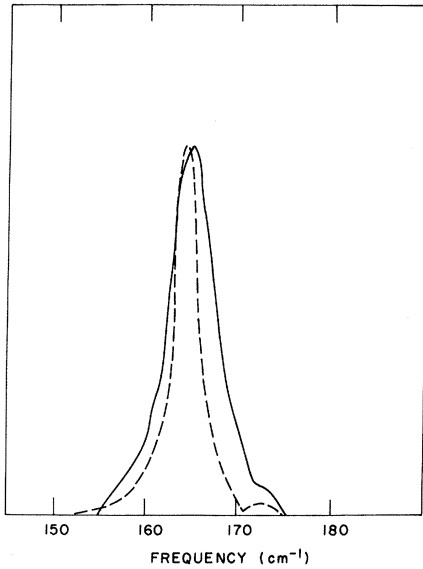


FIG. 4. Raman mode $s_0 + d_{xy}$ from Ni:MnF₂. The experimental data are from Ref. 34. The solid line is experimental and the dashed line theory.

net effect is zero. This situation changes when an impurity is present which may have a g factor g' different from that of the host. The g factors for the s_0 and $s_0 + s_0$ modes were discussed in Sec. IV, based on a cluster model. The g factor for the s_0 mode from Green's-function theory is given by Eq. (18) and the g factor for the $s_0 + s_0$ will be just

$$\begin{aligned} g_{s_0+s_0} &= g_{s_0} + g' = 2g' - (g - g')S'/(Sz - S') \\ &= 2g' - \frac{(g - g')S'}{(Sz - S')} \end{aligned} \quad (54)$$

This expression is valid only for $S' = 1$ when the g factor of the second s_0 is simply g' because the mode is entirely localized within our approximation [Eq. (40)]. The expressions for g_{s_0} and $g_{s_0+s_0}$ from the two theories are rather different in the term proportional to $(g - g')$. This term contains useful information about the spatial extent of the modes [Eq. (19)]. Unfortunately, for Ni:MnF₂, $g = 2.00$ ³⁷ and $g' = 2.33$,³⁸ so that terms in $(g - g')$ are ~ 0.02 , which is too small to observe experimentally²⁰ where the resolution is ± 0.04 .

The g factors for the pair modes $s_0 + \alpha$ are simply given by

$$\begin{aligned} g_{s_0+\alpha} &= g_{s_0} - g = -(g - g')[1 + S'/(Sz - S')] \\ &= -(g - g')[1 + S'/(Sz - S')] \end{aligned} \quad (55)$$

because the α mode is entirely on the host sites.

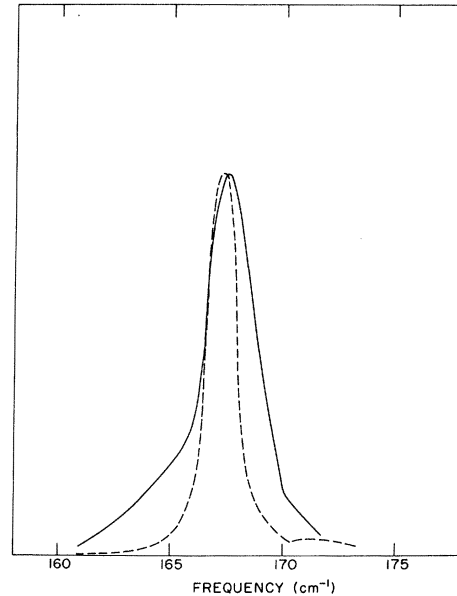


FIG. 5. Infrared absorption $s_0 + f$ from Ni:MnF₂. The experimental data are from Ref. 35 which is a transmission experiment. The background has been subtracted by eye to obtain the solid experimental curve above. The dashed line is theory.

Again the experimental data²⁰ are not accurate enough to determine if the second term in the bracket is present. Some experiments on systems where g and g' had opposite signs so that $(g - g')$ were large would be useful, since the effect of the magnon-magnon interaction on the g factor would be magnified.

X. CONCLUSIONS

We have shown that the pair modes in Ni-doped manganese salts can be understood because all the modes observed so far involve at least one s_0 mode which is strongly localized at the impurity site. We point out that the theory is applicable in other situations (e.g., Fe^{++} in MnF_2). Our reasons for studying Ni-doped manganese salts were threefold. First, this system has been studied extensively experimentally; second, nickel has the strongest exchange interactions in the transition-metal series³⁹; and third, nickel has spin 1, so it behaves like a vacancy when the lattice contains a single spin deviation on the nickel. This means that we can compare theory and experiment without knowing a great deal about the Ni:Mn exchange in MnF_2 .

ACKNOWLEDGMENTS

I should like to thank R. E. Dietz, G. Parisot, and A. Oseroff for permission to use their experimental results prior to publication. I would also like to thank M. Blume, V. J. Emery, and J. B. Parkinson for discussions at various times.

APPENDIX

We give an alternative derivation of $\tilde{S}^\alpha(\omega)$ [Eq. (44)] from which the cross section $S^{s_0+\alpha}(\omega)$ may be obtained. When the s_0 mode is highly localized we may write the intermediate ground state $|I\rangle$ approximately as

$$|I\rangle = [S'_0/(2S')^{1/2}]|0\rangle. \quad (\text{A1})$$

The second mode α does not have s -type symmetry and thus is not allowed to spread onto the impurity. We can therefore factor out the coordinates of the impurity and form an effective Hamiltonian H_{eff}

$$H_{\text{eff}} = \frac{\langle S'_0 = S' - 1 | H + H' | S'_0 = S' - 1 \rangle}{\langle S'_0 = S' - 1 | S'_0 = S' - 1 \rangle}, \quad (\text{A2})$$

where H and H' are given by Eqs. (1) and (3). From

Eq. (A2) we can write

$$H_{\text{eff}} = \sum_{i \neq 0, j} J_{ij} \tilde{S}_i \cdot \tilde{S}_j + \sum_{\Delta} J'(S' - 1) S_{\Delta}^z, \quad (\text{A3})$$

where the exchange couples only nearest neighbors, but we include the subscripts i, j on J for clarity. This Hamiltonian describes a vacancy with an external magnetic field $-J'(S' - 1)$ acting only on the nearest neighbors of the impurity. If we now write the spin operators in (A3) in terms of the Bose operators [Eq. (4)] and keep only the quadratic terms,

$$H_{\text{eff}} = \sum_{i \neq 0, j} J_{ij} S[a_i^\dagger a_i + b_j^\dagger b_j + a_i^\dagger + b_j^\dagger + a_i b_j] - \sum_{\Delta} J'(S' - 1) b_{\Delta}^\dagger b_{\Delta}. \quad (\text{A4})$$

Equation (A4) is quadratic in the Bose operators and may be solved by finding equations of motion for the Green's functions $\langle\langle a_i; a_i^\dagger \rangle\rangle$ and $\langle\langle b_j; a_1^\dagger \rangle\rangle$:

$$\begin{aligned} \omega \langle\langle a_i; a_i^\dagger \rangle\rangle &= (1/2\pi) \delta_{i1} + \sum_j J_{ij} \langle\langle a_i; a_i^\dagger \rangle\rangle \\ &\quad + \sum_j J_{ij} \langle\langle b_j; a_1^\dagger \rangle\rangle, \quad i \neq 0 \\ &= 0, \quad i = 0; \end{aligned} \quad (\text{A5})$$

$$\begin{aligned} \omega \langle\langle b_j; a_1^\dagger \rangle\rangle &= - \sum_{i \neq 0} J_{ij} S \langle\langle b_j; a_1^\dagger \rangle\rangle \\ &\quad - \sum_{i \neq 0} J_{ij} S \langle\langle a_i; a_1^\dagger \rangle\rangle \\ &\quad - J'(S' - 1) \langle\langle b_j; a_1^\dagger \rangle\rangle \delta_{j, \Delta}. \end{aligned} \quad (\text{A6})$$

The coupled equations (A5) and (A6) may be solved in the standard way by forming a Dyson equation⁹ and using the fact that the potential is short ranged. The solution for the non- s -like modes is given by

$$\sum_{i=1} f_{\alpha}(i-1) \langle\langle a_i; a_1^\dagger \rangle\rangle = \frac{1}{2\pi} \left(\frac{G_0^{\alpha}(\omega)}{1 - [J'(S' - 1) - JS] G_0^{\alpha}(\omega)} \right), \quad (\text{A7})$$

[where the $G_0^{\alpha}(\omega)$ are given by Eq. (10) for the perovskite structure and by Eqs. (49)–(51) for the rutile structure. The factors $f_{\alpha}(i-1)$ that select the correct symmetry combinations for the α mode were introduced in Eq. (34). The $\tilde{S}^\alpha(\omega)$ are proportional to the imaginary part of Eq. (A7). Comparing Eq. (A7) with Eq. (9), where ρ is defined in Eq. (6), we see that the impurity acts as if it had a spin $S' - 1$ when the lattice contains a single s_0 mode.] The factor $[J'(S' - 1) - JS]$ is just that used in Sec. VIII for the brief discussion of Fe:MnF_2 . (J and J' were written J_2 and J'_2 in the more conventional notation for the rutile structure.)

[†]Work performed under the auspices of the U. S. Atomic Energy Commission.

¹J. M. Lifshitz, J. Phys. USSR **7**, 215 (1943).

²J. B. Parkinson, Solid State Commun. **5**, 419 (1967).

³T. Wolfram and J. Callaway, Phys. Rev. **130**, 2207 (1963).

⁴S. W. Lovesey, J. Phys. C **1**, 102 (1968).

⁵T. Tonegawa, thesis, Osaka University, 1968 (un-

published).

⁶T. Tonegawa and J. Kanamori, Phys. Letters **21**, 130 (1966).

⁷M. F. Thorpe, Phys. Rev. Letters **23**, 472 (1969).

⁸R. J. Elliott, M. F. Thorpe, G. Imbusch, R. Loudon, and J. B. Parkinson, Phys. Rev. Letters **21**, 147 (1968).

⁹R. J. Elliott and M. F. Thorpe, J. Phys. C **2**, 1630

(1969).

¹⁰C. Kittel, *Quantum Theory of Solids* (Wiley, New York, 1963), Chap. 4.

¹¹J. B. Parkinson, *J. Phys. C* **2**, 2003 (1969).

¹²M. Yussouff and J. Mahanty, *Proc. Phys. Soc. (London)* **85**, 1223 (1965).

¹³D. Hone, H. B. Callen, and L. R. Walker, *Phys. Rev.* **144**, 283 (1966).

¹⁴C. G. Windsor and R. W. H. Stevenson, *Proc. Phys. Soc. (London)* **87**, 501 (1966).

¹⁵S. J. Pickart, M. F. Collins, and C. G. Windsor, *J. Appl. Phys.* **37**, 1055 (1966).

¹⁶L. F. Johnson, R. E. Dietz, and H. J. Guggenheim, *Phys. Rev. Letters* **17**, 13 (1966); A. Missetich and R. E. Dietz, *ibid.* **17**, 392 (1966).

¹⁷A. Oseroff, P. S. Pershan, and M. Kestigian, *Phys. Rev.* **188**, 1046 (1969).

¹⁸The matrix elements of \tilde{S} within a particular \mathbb{S} multiplet are proportional to the matrix elements of \tilde{S} by the Wigner-Eckart theorem. The constant of proportionality is a 6_j symbol that may be evaluated explicitly.

¹⁹The difference between the Holstein-Primakoff transformation and the cluster model is best illustrated in the two-spin Hamiltonian $H = J\tilde{S}_1 \cdot \tilde{S}_2$. The exact separation between the two lowest sets of states if $S_1 \geq S_2$ is $J(S_1 - S_2 + 1)$, whereas the equivalent energy in the Hamiltonian

$$H = J[S_1 a_2^\dagger a_2 + S_2 a_1^\dagger a_1 + \sqrt{S_1 S_2} (a_1^\dagger a_2^\dagger + a_1 a_2)]$$

is $J(S_1 - S_2)$. If we now imagine \tilde{S}_1 to be the total spin of the z nearest neighbors of the impurity and \tilde{S}_2 to be the impurity spin, we can see that quadratic Bose Hamiltonian underestimates the energy of the s_0 mode when the impurity-host exchange is much larger than any other interactions present.

²⁰R. F. Dietz, G. Parisot, A. E. Meixner, and H. J. Guggenheim, *J. Appl. Phys.* **41**, 888 (1970).

²¹P. A. Fleury and R. Loudon, *Phys. Rev.* **166**, 514 (1968).

²²W. J. L. Buyers, R. A. Cowley, T. M. Holden, and R. W. Stevenson, *J. Appl. Phys.* **39**, 1118 (1968).

²³S. J. Allen, Jr., R. Loudon, and P. L. Richards, *Phys. Rev. Letters* **16**, 463 (1966).

²⁴The notation follows that of S. F. Koster, J. O. Dimmock, R. G. Wheeler, and H. Statz, *Properties of the 32 Point Groups* (MIT Press, Cambridge, Mass., 1963).

²⁵M. Wortis, *Phys. Rev.* **132**, 85 (1963).

²⁶E. Frikkee, *Proc. Phys. Soc. (London)* **C 2**, 345 (1969); R. M. White and C. M. Hogan, *Phys. Rev.* **167**, 480 (1968).

²⁷A. Oseroff and P. S. Pershan *Phys. Rev. B* **1**, 2359 (1970).

²⁸P. Moch, G. Parisot, R. E. Dietz, and H. J. Guggenheim (unpublished).

²⁹R. E. Dietz (private communication).

³⁰E. Shiles and D. Hone (unpublished).

³¹A. Okazaki, K. C. Turberfield, and R. W. H. Stevenson, *Phys. Letters* **8**, 9 (1964).

³²O. Nikotin, P. A. Lindgard, and O. W. Dietrich, *J. Phys. C* **2**, 1168 (1969).

³³M. F. Thorpe, *J. Appl. Phys.* **41**, 892 (1970).

³⁴P. Moch, G. Parisot, R. E. Dietz, and H. J. Guggenheim, *Phys. Rev. Letters* **21**, 1596 (1968).

³⁵G. Parisot (private communication).

³⁶R. Weber, *Phys. Rev. Letters* **21**, 1260 (1968).

³⁷M. Tinkham, *Proc. Roy. Soc. (London)* **A236**, 535 (1956).

³⁸M. Peter and J. B. Mock, *Phys. Rev.* **118**, 137 (1960).

³⁹See, for example, Table IV of M. T. Hutchings, M. F. Thorpe, R. J. Birgeneau, H. J. Guggenheim, and P. A. Fleury, *Phys. Rev. B* **2**, 1362 (1970).

Ising Model with Antiferromagnetic Next-Nearest-Neighbor Coupling. II. Ground States and Phase Diagrams*

J. Stephenson and D. D. Betts

Theoretical Physics Institute, University of Alberta, Edmonton, Alberta, Canada

(Received 5 February 1970)

The critical values of the ratio of interaction energies at which the ordering of spins in the ground state is indeterminate (and probably $T_c = 0$) are calculated exactly for a variety of Ising lattices with antiferromagnetic next-nearest-neighbor coupling, and for anisotropic nearest-neighbor coupling. Using these results and the exact two-dimensional solutions, the general dependence of the critical point on interaction ratio is sketched. The complex case of the antiferromagnetic fcc is reconsidered.

The effects of introducing higher neighbor interactions in an Ising model have been investigated recently by series expansion methods,¹⁻³ by exact two-dimensional solutions^{4,5} and by closed-form approximations.⁶⁻⁸ One of the problems is to determine the

dependence of the critical point (Curie point T_c) on the strength and sign of the next-nearest-neighbor interaction. It is generally expected that an antiferromagnetic next-nearest-neighbor interaction will depress the critical point, and if sufficiently